

Diffusion Features to Bridge Domain Gap for Semantic Segmentation

Yuxiang Ji¹, Boyong He¹, Chenyuan Qu², Zhuoyue Tan¹, Chuan Qin³, Liaoni Wu¹

¹ Xiamen University, ² University of Birmingham, ³ The University of Melbourne

yuxiangji@stu.xmu.edu.cn, wuliaoni@xmu.edu.cn

Abstract

Pre-trained diffusion models have demonstrated remarkable proficiency in synthesizing images across a wide range of scenarios with customizable prompts, indicating their effective capacity to capture universal features. Motivated by this, our study delves into the utilization of the implicit knowledge embedded within diffusion models to address challenges in cross-domain semantic segmentation. This paper investigates the approach that leverages the sampling and fusion techniques to harness the features of diffusion models efficiently. Contrary to the simplistic migration applications characterized by prior research, our finding reveals that the multi-step diffusion process inherent in the diffusion model manifests more robust semantic features. We propose Diffusion Feature Fusion (DIFF) as a backbone use for extracting and integrating effective semantic representations through the diffusion process. By leveraging the strength of text-to-image generation capability, we introduce a new training framework designed to implicitly learn posterior knowledge from it. Through rigorous evaluation in the contexts of domain generalization semantic segmentation, we establish that our methodology surpasses preceding approaches in mitigating discrepancies across distinct domains and attains the state-of-the-art (SOTA) benchmark. Within the synthetic-to-real (syn-to-real) context, our method significantly outperforms ResNet-based and transformer-based backbone methods, achieving an average improvement of 3.84% mIoU across various datasets. The implementation code will be released soon.

Keywords

Diffusion Models, Domain Generalization, Semantic Segmentation

1 Introduction

The paradigm of training semantic segmentation models on large-scale datasets has demonstrated significant successes; nevertheless, the obstacles associated with the acquisition of data specific to niche scenarios, coupled with the labor-intensive nature of manual annotation, continue to pose significant challenges. Synthetic data, while annotated by construction and complementing some missing data, usually suffers from the issue of domain gaps. This issue arises because models trained on limited synthetic data tend to have a substantial decline in accuracy when applied in real-world settings, attributable to domain shifts in the test data [52, 62]. Research has shown that one of the important factors is the representation discrepancy caused when the perspective, background, style, or imaging conditions of the image are changed to the unseen domain [11, 12, 33]. As illustrated in Fig. 1, the urban road scene data from different scenarios undergoes varying degrees of distribution discrepancy after image encoding, which has been pre-trained on

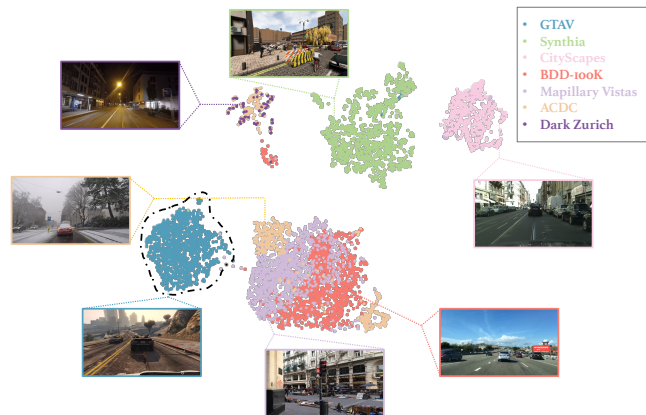


Figure 1: Visualization of domain gap by UMap [30] embedding of the backbone features on seven synthetic and real-world urban road scene datasets. The backbone is MiT-B5 [55] pre-trained on ImageNet. The dash-dot line is the synthetic dataset GTAV [39].

ImageNet. If a conventional training approach is employed, focusing solely on the readily available synthetic dataset GTAV [39], the model will adequately fit this narrow distribution range, subsequently losing its capacity for generalized modelling of unseen scene data. Taking this issue, the study of Domain Generalization (DG) study focuses on reducing the domain variance performance and improving the model robustness across unseen domains.

Recently, the stunning performance of diffusion models on various tasks of image generation has attracted a great deal of research attention. The central focus of such research and application is the text-to-image diffusion model (e.g., Stable Diffusion [40]) trained on large-scale text-image pairs datasets. The large-scale trained text-to-image diffusion model possesses the capability to synthesis images of remarkable realism and high quality across diverse styles, scenes, and categories, contingent upon the customized prompts given. This indicates that the diffusion model learns generic visual features while being able to disentangle the representations of image features according to conditional text inputs. Several studies also validate the ability of pre-trained diffusion models on representational and perceptual tasks [2, 7, 28, 32, 48, 59]. Drawing inspiration from the implicit universal knowledge embedded within pre-trained diffusion models, it leads us to think: **how to utilize such knowledge to reduce the domain discrepancy in semantic segmentation?**

The core capability of diffusion models, the step-by-step diffusion denoising process, is carried out by its critical component, U-Net [41]. Therefore, our research also focuses on U-Net, a point

that is validated by some previous works [2, 28, 59]. Unlike the usual generative tasks where the noise predicted by U-Net is gradually removed, we need to extract features from a clean input image. Our strategy performs an inverse process, where the predicted noise is gradually added to the input image. Different from similar studies that use single-step denoising for extracting features, we consider the diffusion trajectory as a more meaningful feature. In this way, we propose **Diffusion Feature Fusion (DIFF)** to collect and integrate the feature sets of the whole diffusion process. Among them, we use the intermediate latent variables in the U-Net decoder and the cross-attention maps as the feature collection sets to build an interactive understanding of visual perception and text semantics in the pre-trained diffusion model. Then the extracted feature sets will be fused by a fusion network to align the standard perception image encoder and can be used as a normal backbone for semantic segmentation. To further utilize the conditional generation capability of the pre-trained diffusion model and to address the absence of corresponding annotation text as conditional input when doing prediction, we introduce a special implicit posterior knowledge learning framework for supervised learning. Our main idea and network structures are visible in Fig. 2 and Fig. 3. With the benefit of the training framework, semantic segmenting networks are able to implicitly learn posterior knowledge from the conditional generative capabilities of the diffusion model. This approach, based on a multi-modal learning paradigm integrating language and visual features, guides the model to acquire more generalized representations, thereby enhancing its generalization capabilities when confronted with unseen data.

To validate the effectiveness of our method in mitigating the effect of domain discrepancy on semantic segmentation, we do the evaluations under the DG setting around datasets with varying degrees of domain differentiation. With the proposed DIFF and training framework, we establish new state-of-the-art (SOTA) results on domain generalization semantic segmentation, achieving an average improvement of 3.84% mIoU. This is more pronounced in the data with greater domain differences among it, with a boost of 8% mIoU.

Our contributions are summarized as follows:

- We exploit the generalized representation capability of pre-trained diffusion models for cross-domain semantic segmentation.
- We study the impact of the diffusion sampling process and the composition of the diffusion model’s components on representational capabilities, and propose **Diffusion Feature Fusion (DIFF)** for extracting and fusing diffusion trajectory features.
- We introduce an implicit posterior knowledge learning framework for leveraging the conditional generation capability of the pre-trained diffusion model.
- Our method reaches a new SOTA domain generalization semantic segmentation performance on GTAV to five real-world datasets of an average of 49.69% mIoU, which exceeds the previous method by 3.84% mIoU.

2 Related Work

Domain Generalization Semantic Segmentation. To alleviate the degradation of model transferability caused by the domain gap in semantic segmentation, methods aimed at enhancing

the model generalization performance are being explored. Some domain adaptation research focuses on learning to perform the same task in a visible unannotated target domain from a similar source domain [17, 50]. For a more general setting, Domain Generalization (DG) assumes the task of learning from limited visible data for effective performance in unseen target domains within the same task group [31, 33]. To enhance the generalization of model across domains, numerous methods [8, 12, 29, 33, 35] remove domain-related components through whitening or normalization, and try to align the features of different domains so that the network can learn domain-invariant knowledge. Another line of study [18, 19, 23, 38, 60, 61] focuses on how to extend the source domain through domain randomization, aiming to broaden the model performance on more general domains. DAFormer [17] and CMFormer [4] find that the natural robustness of the dynamic computation of self-attention in transformer-based methods is more suitable for domain generalization semantic segmentation learning. Especially, [14, 36] utilize diffusion model to generate cross-domain images for training to enhance model cross-domain performance for semantic segmentation. Instead of the generation-then-training paradigm, our method directly exploits the proficiency of the diffusion model in cross-domain image representation.

Diffusion Model Representations. As diffusion models have great success in generative tasks, researchers attempt to analyze underlying representations inside the model. [22, 27] manipulate the resultant effect by regulating the latent representation within the diffusion model. There are also several studies that explore the potential of diffusion models on perceptual tasks. DIFT [48] extracts the diffusion feature in a one-step pipeline manner for semantic matching, while DiffHyperfeatures [28] explores the way of aggregating multi-step features. DDPMSeg [2] and ODISE [56] demonstrate the capabilities of diffusion representations for semantic segmentation. Particularly, PromptDiff [13] is the most related work to our method, which attempts to utilize the diffusion model as a backbone on domain generalized semantic segmentation. However, it directly takes off-the-shelf pre-trained diffusion models, lacking exploration on how to obtain features that are more meaningful for perception. In contrast, we combine studies of diffusion modelling features [6] and component effect [7], to propose a feature extraction and fusion structure that is more suitable for semantic segmentation. The other two recent related works are VPD [59] and DiffSegmenter [53], which also explore utilizing the interaction of text prompts with the visual perception of diffusion model in segmentation, yet they lack research on prediction scenarios without conditional input guidance. We introduce a special training framework to implicitly learn a posterior knowledge of the pre-trained conditional diffusion model, and extend the capability to the case of predictions without conditional inputs.

3 Method

In Sec. 3.1, we will first review the background of the diffusion model, and revisit the diffusion process from the perspective of trajectory. Then in Sec. 3.2, we will present our feature extraction and fusion approach **Diffusion Feature Fusion (DIFF)** based on the diffusion process. We will introduce an implicit posterior learning framework for leveraging the conditional generation knowledge

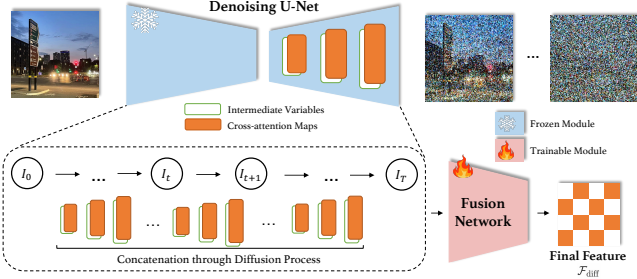


Figure 2: Illustration of Diffusion Feature Fusion (DIFF). Only the fusion network is trained while the denoising U-Net is frozen.

of the pre-trained diffusion model in Sec. 3.3, accompanied by the study on the sampling schedule in Sec. 3.4.

3.1 Preliminaries

Diffusion model [16, 47] is set up to model a process that gradually removes noise from a standard noise distribution to an image distribution. To simulate such a process for training, Gaussian noise would be gradually added proportionally to a clean image until it becomes completely noisy, which is called the “forward diffusion process”:

$$x_t = \sqrt{\alpha_t}x_0 + \sqrt{1 - \alpha_t}\epsilon, \quad \epsilon \in \mathcal{N}(\mathbf{0}, \mathbf{I}), \quad (1)$$

where $t \in [0, T]$ denotes the number of diffusion steps in a discrete sense. $\{\alpha_t\}$ are the coefficients of the noise scheduler, which could be considered as the stepsize of each diffusion step.

For model training, the objective is typically constructed by re-parameterizing as:

$$\mathbb{E}_{x_0, \epsilon, t} [\|\epsilon - \epsilon_\theta(x_t, t; C)\|], \quad (2)$$

where ϵ_θ is usually implemented through an U-Net of shared parameters for t . C represents the condition input for the conditional generation, which is generally fused with the layers of features via cross-attention [5, 40]. When doing pre-training in the text-to-image paradigm, the condition input $C = y$ will be encoded to the text embedding $E_\theta(y) \in \mathbb{R}^{M \times E}$ by the text encoder E_θ , then mapped to the U-Net intermediate layers via an attention layer as $\text{Attention}(Q, K, V) = \text{softmax}(\frac{QK^T}{\sqrt{d}}) \cdot V$ with

$$Q = W_Q^{(i)} \cdot \varphi_i(z_t), \quad K = W_K^{(i)} \cdot E_\theta(y), \quad V = W_V^{(i)} \cdot E_\theta(y), \quad (3)$$

where z_t represents the intermediate variables of U-Net, $\varphi_i(z_t) \in \mathbb{R}^{N \times d_i^i}$ denotes the flattened representation of z_t . $W_Q^{(i)}, W_K^{(i)}, W_V^{(i)}$ are learnable projection metrics [20, 51]. In such a structure, we refer to the intermediate latent variables at each layer l and each timestep t during the prediction phase of the U-Net decoder as $\mathcal{V}_{t,l}^{\text{inter}}$, and the results of the cross-attention as $\mathcal{A}_{t,l}^{\text{cross}}$.

From a continuous state-space perspective, the training objective implicitly fits the score (gradient of the log probability density with respect to data) with various levels of noise [47]. Corresponding back to the discrete setting, the step-by-step diffusion sampling process can be viewed as a trajectory in the direction of the score [6].

3.2 Diffusion Feature Fusion

By reviewing the mechanics of diffusion models, we could learn that the diffusion model removes the noise from the pure noise distribution step by step through its core prediction network U-Net to fit the image distribution. In such a denoising generation process, the model needs to comprehend the image itself, implying an underlying modelling of the visual aspects. The embedded knowledge exists in the set of intermediate features, which runs through the layers of the U-Net with each step of diffusion, and it was found that different pairs of layers and steps implied different meaningful features [2, 48].

Combined with the previous understanding of the diffusion process, the complete process of the diffusion model consists of multiple steps, or in other words, a trajectory. To maximize the utilization of the knowledge implicit within the diffusion model, we consider extracting the latent variables at each step and layer during the diffusion process, utilizing them as trajectory features. In alignment with the architectural design and pre-training scheme, we devise two distinct feature sets from U-Net aimed at facilitating the integration of visual and text semantic understanding. Specifically, we extract the intermediate latent variables $\{\mathcal{V}_{t,l}^{\text{inter}}\} \in \mathbb{R}^{d_l \times w_l \times h_l}$ from each layer l and each step t within the U-Net decoder as the visual representation, and the cross-attention maps $\{\mathcal{A}_{t,l}^{\text{cross}}\} \in \mathbb{R}^{d_l \times w_l \times h_l}$ as the interaction representations between visual and text content.

However, directly taking out the features of the whole process layer by layer would lead to too numerous and unwieldy for practical utilization, which is also the reason that many works apply a one-step diffusion pipeline and hand-select the block, step pairs by grid search. Inspired by DiffHyperfeature [28], here we proposed DIFF (**D**iffusion **F**eature **F**usion) to fuse features extracted from different layers with different steps by an aggregating network. Moreover, the researches on image style transfer tasks [54] find that altering the generated effects can be achieved by specifying different steps of the diffusion process. From this perspective, we could consider that the model’s understanding of images varies at different steps, or in other words, the direction of each step in the diffusion trajectory could represent different information. Therefore, our DIFF method fuses both temporal and spatial dimensions simultaneously, rather than through a simple summation or weighted average, which would compromise the independence of features at different steps. The final DIFF features $\mathcal{F}_{\text{diff}}$ are aggregated by a fusion network F :

$$\mathcal{F}_{\text{diff}} = F(\oplus_{t,l} [\mathcal{V}_{t,l}^{\text{inter}}, \mathcal{A}_{t,l}^{\text{cross}}]), \quad (4)$$

where $\oplus_{t,l}$ means the concatenation across t and l .

3.3 Implicit Posterior Knowledge Learning

If the unconditional generative capability represents the understanding of low-level image details from the diffusion model, then the text-to-image conditional generative capability represents the mastery of high-level knowledge from language to image. We could consider a pre-trained conditional diffusion model as modelling the gradients of data density $\nabla_{x_t} \log p(x_t|C)$ [3], or in other words, it possesses knowledge $p(x|C)$. Several studies [21, 43, 54] discover the uncouplability of text control, i.e., we can control the environment, weather, style, background, etc. of the generated image by

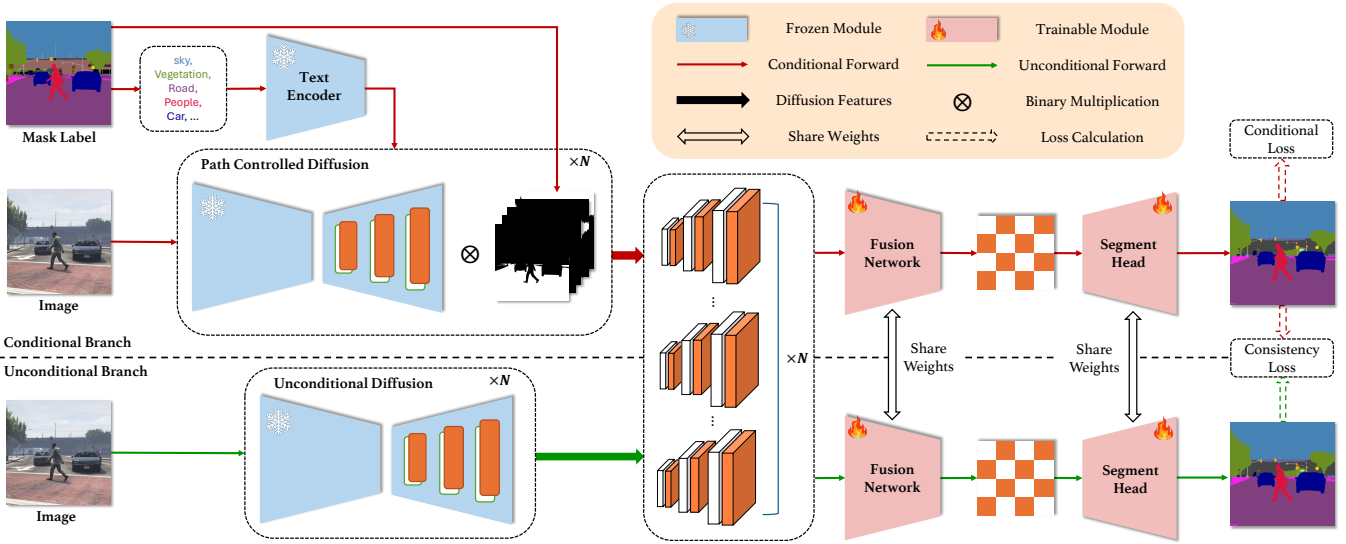


Figure 3: Overview of implicit posterior knowledge learning framework. (a) In the conditional branch, we extract the categories and masks from the semantic segmentation annotations and use them as conditions, which are input into the diffusion model along with the input image. Through the DIFF module, we obtain features enhanced with conditional information for supervised training. (b) In the unconditional branch, we only use the image as input to the DIFF module and employ the prediction results from the conditional branch as a teacher for consistency loss.

changing the definiteness of the prompt, which is precisely a cross-domain capability. Motivated by this, our objective is to leverage from the prior conditional knowledge $p(\mathbf{x}|\mathbf{C})$ of pre-trained diffusion model to the **posterior knowledge** $p(\mathbf{C}|\mathbf{x})$. While we discuss the utilization of diffusion models for image modelling and visual language associations in Sec. 3.2, we overlook an important issue, namely, **how to add text conditional input in the supervised learning paradigm?**

For semantic segmentation, if we let $\{\mathbf{x} \in \mathbb{R}^{3 \times w \times h}, \mathbf{y} \in \mathbb{R}^{w \times h}\}$ be the set of images and mask labels, the task of a segmentor D is to learn $p(\mathbf{y}|\mathbf{x})$. Combing our previous discussion on diffusion features, the entire task can be decomposed into $p(\mathcal{F}_{\text{diff}}|\mathbf{x})$ and $p(\mathbf{y}|\mathcal{F}_{\text{diff}})$, where $p(\mathcal{F}_{\text{diff}}|\mathbf{x})$ is done by DIFF, and $p(\mathbf{y}|\mathcal{F}_{\text{diff}})$ is done by segmenting head. To integrate conditional generation into our DIFF method, during the training process, we decompose the semantic segmentation labels \mathbf{y} into multiple groups of masks $M \in \{0, 1\}^{\text{cls} \times w \times h}$ and their corresponding category descriptions $c \in \{\text{sky}, \text{vegetation}, \text{road}, \text{people}, \text{car}, \dots\}^{\text{cls}}$, where cls represents the number of all categories. Following the training-free method MultiDiffusion [1], we control the diffusion sampling path by

$$I_{t+1}(I_t, M, c) = \sum_{i=1}^{\text{cls}} \frac{M_i}{\sum_{j=1}^{\text{cls}} M_j} [M_i \otimes (\Phi(I_t, c_i))], \quad (5)$$

where Φ represents the pre-trained text-to-image diffusion model. We name this process by path-controlled diffusion as shown in the conditional branch in Fig. 3. Intriguingly, when we do the training with conditional branch to obtain conditional feature $\mathcal{F}_{\text{diff}}^{\text{con}}$, the segmenting head $p(\mathbf{y}|\mathcal{F}_{\text{diff}}^{\text{con}})$ exhibits better performance on both training metrics and prediction results across source and unseen

domain. This indicates that through conditional generative capabilities $p(\mathbf{x}|\mathbf{C})$, the latent representations of the diffusion model display more meaningful features $\mathcal{F}_{\text{diff}}^{\text{con}}$ for segmentation. Similar to Bayesian learner, the segmentation network intricately acquires posterior knowledge $p(\mathbf{y}|\mathcal{F}_{\text{diff}}^{\text{con}})$ through an implicit way facilitated by the utilization of pre-trained diffusion model knowledge $p(\mathcal{F}_{\text{diff}}^{\text{con}}|\mathbf{x}, \mathbf{C})$. The learning objective of the conditional branch could be seen as a normal semantic segmentation target

$$\mathcal{L}_{\text{condit}} = \text{CE}(D(\mathcal{F}_{\text{diff}}^{\text{con}}), \mathbf{y}). \quad (6)$$

Although $\mathcal{F}_{\text{diff}}^{\text{con}}$ displays more meaningful features compared to $\mathcal{F}_{\text{diff}}^{\text{uncon}}$, we are still unable to obtain the mask labels \mathbf{y} when doing predictions, thus we cannot convert them into conditional inputs \mathbf{C} . To address this issue, we set up an additional unconditional branch as shown in 3. In this branch, the diffusion features $\mathcal{F}_{\text{diff}}^{\text{uncon}}$ are acquired with DIFF through an unconditional process $p(\mathcal{F}_{\text{diff}}|\mathbf{x}, \mathbf{C} = \emptyset)$. We could attribute segmenting network in conditional branch modeling the distribution $p(\mathbf{y}|\mathbf{x}_{\text{img}}, \mathbf{x}_{\text{text}})$, while the unconditional branch modeling the distribution $p(\mathbf{y}|\mathbf{x}_{\text{img}})$. In order to bring the superior performance of the conditional branch to the unconditional branch, we aim to make the two branches as consistent as possible:

$$p_{\text{uncon}}(\mathbf{y}|\mathbf{x}_{\text{img}}) \sim p_{\text{con}}(\mathbf{y}|\mathbf{x}_{\text{img}}, \mathbf{x}_{\text{text}}). \quad (7)$$

We align the segmenting head $p(\mathbf{y}|\mathcal{F}_{\text{diff}}^{\text{con}})$ and $p(\mathbf{y}|\mathcal{F}_{\text{diff}}^{\text{uncon}})$ by simply employing an L2 (least square error) loss for a consistency study between the outputs of two branches as

$$\mathcal{L}_{\text{consis}} = \|D(\mathcal{F}_{\text{diff}}^{\text{con}}), D(\mathcal{F}_{\text{diff}}^{\text{uncon}})\|_2. \quad (8)$$

In this way, the implicit posterior knowledge learned from the conditional generative model could be gradually distilled onto the unconditional input branch. The complete learning objective is the

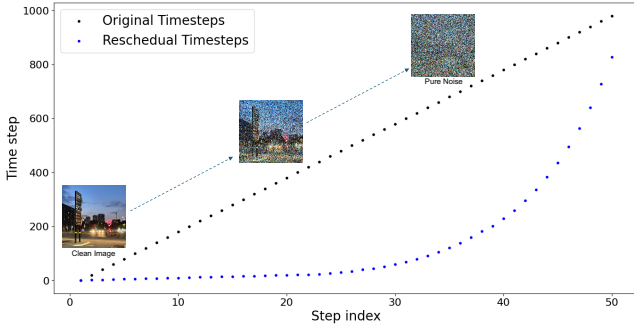


Figure 4: Timestep re-schedules. The original timesteps are scheduled as a linear sub-sequence τ from complete $[1, \dots, T]$ [46]. We sample with exponentially increasing step sizes as $\tau_i = ae^{bi}$, focusing more steps on clearer images.

combination of conditional segmentation loss $\mathcal{L}_{\text{condit}}$ and consistency loss $\mathcal{L}_{\text{consis}}$ as

$$\mathcal{L}_{\text{final}} = \lambda_1 \mathcal{L}_{\text{condit}} + \lambda_2 \mathcal{L}_{\text{consis}}. \quad (9)$$

Here, λ_1 and λ_2 are two hyper-parameters to control the weights of two objectives, which are both set to 1 in our experiment.

3.4 Diffusion Sampling Stepsize Re-schedule

To reduce the number of inference steps (typically 1000) for models trained based on DDPM[16] settings, some accelerated sampling methods are proposed: e.g., ODE based method DDIM[46], higher-order based method DPM-Solver [26], pseudo-numerical based method PNDM [24]. These methods employ different methods to force the predictions to converge faster on the data manifolds, the region whose higher log density. Back to our task, since the need to get meaningful representations from an input image, which is similar to the image editing tasks, we utilize the diffusion inversion pipeline commonly used in it as:

$$x_{\tau_{i+1}} = \sqrt{\alpha_{\tau_{i+1}}} \left(\frac{x_{\tau_i} - \sqrt{1 - \alpha_{\tau_i}} \epsilon_{\theta}^{(\tau_i)}(x_{\tau_i})}{\sqrt{\alpha_{\tau_i}}} \right) + \sqrt{1 - \alpha_{\tau_{i+1}} - \sigma_{\tau_i}^2} \cdot \epsilon_{\theta}^{(\tau_i)}(x_{\tau_i}) + \sigma_{\tau_i} \epsilon_{\tau_i}, \quad (10)$$

where τ is the subsequence of the complete diffusion steps $[1, T]$, determining the step size of the inverse diffusion process. It is obvious that the error would gradually accumulate once it deviates from the data manifolds in the direct inversion process. The error will be progressively exacerbated as the noise component increases (as t approaches T), leading to the emergence of features characterized by semantic confusion. This phenomenon is also discovered in [54].

To mitigate this issue and extract more meaningful latent features, we re-design the step scheduler for the sampling process. Specifically, we let $\{\tau_i\}$ change from linear growth to exponential growth in the range of $[1, T]$. As illustrated in Fig. 4, under such a setup, the diffusion sampling step size gradually increases from small to large. This approach ensures that the extracted features are more concentrated on the front part of the inversion process, which is also when the noise component in the input image is smaller. The change significantly enhances the model’s performance with the DIFF block. This is fundamentally similar to the findings regarding the noise scheduler in [7].

4 Experiments

4.1 Experimental Setup

Given the setup of prior research on domain generalization for semantic segmentation [23, 35, 60], the model trained on a source domain dataset will be evaluated on a series of unknown target datasets. We select a more practically significant category of synthetic-to-real domain pairs as the benchmark for evaluation. Specifically, we use GTAV [39], a dataset consisting of 24,966 images rendered by the GTAV game, and Synthia [42], a dataset with 9,400 virtual city images, as the synthetic source domain. For the conventional unknown real domains, we select three standard urban semantic segmentation datasets. CityScapes (CS) [9], BDD-100K (BDD) [57] and Mapillary Vistas (MV) [34] provide semantic segmentation validation sets with 500, 1000, and 2000 images of real urban street scenes from different cities, respectively. To further demonstrate the effectiveness of our proposed method in mitigating domain gap, we additionally utilize two real-world validation datasets with significant domain disparities: ACDC [45] and Dark Zurich (DZ) [44]. These two datasets include images taken under adverse weather conditions or at night, presenting greater domain differences and generalization challenges. All evaluation metrics are based on the mean Intersection over Union (mIoU/%).

Remark: In tables, the best results are highlighted in **bold**, while the second best is underlined.

4.2 Implementation Details

Our model is based on the pre-trained Stable Diffusion [40] released version v1-5. To build up our DIFF block, we extract the output of each residual layer $l \in [0, 12]$ across inversion timesteps $\{\tau_{i=0}, \dots, \tau_{i=49}\}$, $i \in \{0, 5, 10, 15, 20, 25, 30, 35, 40, 45, 49\}$ from U-Net decoder as intermediate variables $\{\mathcal{V}_{t,l}^{\text{inter}}\}$, and the cross-attention maps $\{\mathcal{A}_{t,l}^{\text{cross}}\}$ for input of the fusion network. The fusion network is built by a simple residual bottleneck [15, 28, 56], to merge the input from two sets of features into the final feature $\mathcal{F}_{\text{diff}}$. For the re-scheduled timesteps, we adopt $a = 1.34$, $b = 0.13$ for $\tau_i = ae^{bi}$ as the generating function to produce an integer sequence with a length of 50 as the inverse diffusion timesteps. Following the decoder and training settings in SegFormer [55] and DAFormer [17], we build our segmentation head and train the whole network with AdamW [25], a learning rate of $\eta = 6 \times 10^{-4}$ and a weight decay of 0.01 for both DIFF block and decoder head. More details are put in supplementary.

4.3 Main Results

In Tab. 1, we compare our method with state-of-the-art DG methods including IBN-Net [35], DRPC [58], ISW [8], FS DR [18], SAN-SAW [37], WildNet [23], SHADE [60], ReVT [49], DAFormer [17], CMFormer [4] and PromptDiff [13] on GTAV source setting. The evaluation is performed on five real-world datasets (CS, BDD, MV, ACDC, DZ), which are used to provide a more comprehensive and convincing cross-domain performance check. From the results, our method improves 11.35%, 9.94%, 14.35%, 21.55%, and 21.00% mIoU compared to the ResNet-101 backbone based methods on five datasets respectively. Compared to the superior transformer-based approaches, our method achieves an average improvement of up

Table 1: Comparison to SOTA DG Methods on GTAV Source Domain. Training is performed on synthetic dataset GTAV [39]. Evaluation is performed on five real-world datasets with 19 categories. The dash symbol ‘-’ denotes cases where either the metric is not reported or the official source code is not released. Avg3 and Avg5 refer to the average results on the first three and first five unseen datasets, respectively.

DG Method	Backbone	mIoU (%) on						
		CS [9]	BDD [57]	MV [34]	Avg3	ACDC [45]	DZ [44]	Avg5
IBN-Net [35]	ResNet-101	37.37	32.29	33.84	33.15	-	-	-
DRPC [58]	ResNet-101	42.53	38.72	38.05	39.77	-	-	-
ISW [8]	ResNet-101	37.20	33.36	35.57	35.38	-	-	-
FSDR [18]	ResNet-101	44.80	41.20	43.40	43.13	24.77	9.66	32.77
SAN-SAW [37]	ResNet-101	45.33	41.18	40.77	42.23	-	-	-
WildNet [23]	ResNet-101	45.79	41.73	47.08	44.87	-	-	-
SHADE [60]	ResNet-101	46.66	43.66	45.50	45.27	-	-	-
ReVT [49]	MiT-B5	49.96	48.01	53.06	50.34	41.15	21.99	42.84
DAFormer [17]	MiT-B5	52.65	47.89	54.66	51.73	38.25	17.45	42.18
CMFormer [4]	Swin-B	<u>55.31</u>	<u>49.91</u>	60.09	<u>55.10</u>	<u>41.34</u>	<u>22.58</u>	<u>45.85</u>
PromptDiff [13]	Diffusion	52.00	-	-	-	-	-	-
Ours	Diffusion	58.01	53.60	<u>59.85</u>	57.15	46.32	30.66	49.69
		+2.70	+3.69	-0.24	+2.05	+4.98	+8.08	+3.84

to 3.84% mIoU over all datasets. The results demonstrate the excellent modelling ability of the diffusion-based approach for universal representations and its efficiency in the mitigation of cross-domain degradation in semantic segmentation. Additionally, compared to PromptDiff [13], which is also a diffusion-based method, our performance on a single dataset surpasses it by 6.01% mIoU. In more detail, our method shows higher improvements (4.98%, 8.08% mIoU) against adversarial environment datasets ACDC [45] and Dark Zurich [44], that data with larger domain discrepancies. This corroborates its capability to reduce domain disparities. It is worth noting that unlike previous approaches that introduce additional complex training mechanisms, such as references for content at different resolutions in CMFormer [4], combinations of results from multiple training schemes in ReVT [49], and extensions of training data in SHADE [60], our approach is end-to-end and does not introduce any reference information.

Furthermore, we extend our evaluation on the synthetic data Synthia [42] as the source domain. The training is performed on Synthia [42], and the evaluation is also performed on five real-world datasets CS, BDD, MV, ACDC, DZ. The results presented in Tab. 2 again confirm that our method has narrowed the distance between domains in cross-domain semantic segmentation. These results affirm the versatility and robustness of our approach.

Tab. 3 shows the results of different Domain Generalization methods on the GTAV [39] to CityScapes [9] settings. Although our method is weaker than transformer-based methods in oracle performance, mainly due to the fixed diffusion part, it demonstrates superior performance both in absolute and relative terms under domain generalization. This further substantiates the significance of our approach for domain generalization.

4.4 Ablation Study and Analysis

In this section, we will conduct detailed ablation studies to analyze the effectiveness of each proposed component.

4.4.1 Components Ablation Study.

The overall ablation experiment is shown in Tab. 4. We observe

Table 2: Comparison to SOTA DG Methods on Synthia Source Domain. Training is performed on synthetic dataset Synthia[39]. Evaluation is performed on five real-world datasets with 16 categories. The dash symbol ‘-’ denotes cases where either the metric is not reported or the official source code is not released. Avg3 and Avg5 refer to the average results on the first three and first five unseen datasets, respectively.

DG Method	Backbone	mIoU (%) on						
		CS [9]	BDD [57]	MV [34]	Avg3	ACDC [45]	DZ [44]	Avg5
IBN-Net [35]	ResNet-101	32.04	30.57	32.16	31.59	-	-	-
DRPC [58]	ResNet-101	35.65	31.53	32.74	33.31	-	-	-
ISW [8]	ResNet-101	35.83	31.62	30.84	32.76	-	-	-
FSDR [18]	ResNet-101	40.80	39.60	37.40	39.30	-	-	-
SAN-SAW [37]	ResNet-101	38.92	35.24	34.52	36.23	-	-	-
DAFormer [17]	MiT-B5	44.08	33.20	42.99	40.09	26.62	14.14	32.21
ReVT [49]	MiT-B5	46.28	<u>40.30</u>	<u>44.76</u>	<u>43.78</u>	<u>35.75</u>	<u>20.10</u>	<u>37.44</u>
CMFormer [4]	Swin-B	44.59	33.44	43.25	40.43	34.50	19.57	35.07
PromptDiff [13]	Diffusion	<u>49.10</u>	-	-	-	-	-	-
Ours	Diffusion	49.31	42.20	49.47	46.99	36.27	23.39	40.13
		+0.21	+1.90	+4.71	+3.21	+0.52	+3.29	+2.69

Table 3: Comparison of mIoU(%) to SOTA transformer-based Domain Generalization methods with generalization performance and oracle performance. DG means that training is performed on GTAV [39], evaluation is performed on CityScapes [9]. Oracle means that training and evaluation are both performed on CityScapes. Relative value represents the relative DG performance wrt. the oracle performance.

DG Method	Backbone	DG	Oracle	Relative
DAFormer [17]	MiT-B5	52.65	75.89	69.38%
ReVT [49]	MiT-B5	49.96	75.63	66.06%
CMFormer [4]	Swin-B	55.31	81.85	67.57%
Ours	Diffusion	58.01	74.87	77.17%

that even the diffusion baseline without any optimization methods beats all ResNet-based domain generalization methods, and is also competitive with some transformer-based approaches. This indicates the ability of pre-trained diffusion models to encapsulate and represent universal characteristics for cross-domain images. Combined with DIFF, the diffusion-based backbone could capture the features of the entire diffusion process, utilizing information about the diffusion trajectory, which brings a +5.08% mIoU enhancement. To prevent the inverse diffusion process from being biased towards regions of meaningless noise, timestep rescheduling improves model performance by +1.48% mIoU. Implicit posterior knowledge learning further leverages the pre-trained conditional generating capacity, and converts part of the pre-training knowledge into the perception ability of the segmentation network. This leads to another +1.73% mIoU boost. We also measure the impact of the proposed method on category-IoU as shown in Fig. 5. From the heatmap, it can be observed that the results, which combine all proposed methods, exhibit a notable improvement in generalization performance compared to the baseline across the categories of *sidewalk*, *wall*, *traffic light*, *bus*, and *train*. This suggests the effectiveness of our proposed components in bridging the domain gap.

4.4.2 Diffusion Feature Extraction and Fusion Study.

We evaluate the effectiveness of the proposed component DIFF on

Table 4: Main Ablation Study on the different proposed components. The baseline is set to the one-step inverse diffusion pipeline, without any feature aggregation method. Training is performed on the synthetic dataset GTAV[39]. Evaluation is performed on the three real-world datasets.

DIFF	Timestep Re-schedule	Implicit Knowledge Learning	mIoU (%) on CS
-	-	-	49.72
✓	-	-	54.80
✓	✓	-	56.28
✓	✓	✓	58.01

	- Road	- S.walk	- Build.	- Wall	- Fence	- Pole	- T.Light	- T.Sign	- Veget.	- Terrain	- Sky	- Person	- Rider	- Car	- Truck	- Bus	- Train	- M.cycle	- Bike	- mIoU
Baseline	91	53	85	33	40	46	38	35	87	43	90	61	33	86	42	46	2	21	20	49
+ DIFF	94	56	88	44	46	52	51	33	88	51	86	67	37	89	40	59	5	27	29	54
+ Step Sched.	95	54	88	45	47	51	51	38	88	43	85	66	35	90	44	59	16	28	30	56
+ IPKL	96	65	88	51	45	51	42	89	49	88	88	67	36	89	52	64	22	30	31	58

Figure 5: Comparison of category-wise IoU between performance with different proposed components. Training is performed on GTAV[39]. Evaluation is performed on CityScapes[9]. The color visualizes the difference from the baseline.

Sec. 3.2. As we have discussed, we propose that the fusion of feature variables from a multi-step diffusion process can be more effectively utilized to model image representations during pre-training of diffusion models. Here we use the one-step inverse diffusion pipeline without any aggregation method as a baseline. We also compare with a weighted average method introduced by DiffHyperfeature [28], which aggregates the diffusion features from different timesteps by a learnable weighting parameter. Furthermore, we examine the effect of combining different features in the diffusion model. Tab. 5 shows that the one-step baseline method lags behind all methods with the multi-step process. The DIFF method outperforms the weighted average method 0.74% mIoU, demonstrating better modelling and integration of the diffusion trajectory. The method that incorporates cross-attention maps $\mathcal{A}_{t,l}^{\text{cross}}$ surpasses the method that only includes intermediate variables $\mathcal{V}_{t,l}^{\text{inter}}$.

4.4.3 Implicit Posterior Knowledge Learning Study.

We evaluate the effects of implicit posterior knowledge learning (IPKL) and different consistency losses on the overall results on Tab. 6. The results indicate that employing L2 as a consistency loss in the implicit posterior knowledge learning approach can further enhance the cross-domain performance of our method. This also demonstrates that through the implicit posterior knowledge learning approach, we can transform a portion of the conditional generative capability $p(x|C)$ of a pre-trained diffusion model into the perceptual ability $p(y|x)$ of a segmentation network. The implicit posterior knowledge learning method without consistency loss training will instead degrade the performance of the network due to the fact that there is no conditional input for prediction. In this way, the network not only fails to learn the pre-trained implicit knowledge, but also loses performance due to the inability to grasp the unconditional feature distribution because of the

Table 5: Diffusion Feature Extraction and Fusion Study The baseline is set to the one-step inverse diffusion pipeline, without any feature aggregation method. $\mathcal{V}_{t,l}^{\text{inter}}$ represents intermediate variables of U-Net decoder, and $\mathcal{A}_{t,l}^{\text{cross}}$ represents the cross-attention maps. Weighted average refers to the aggregation method in DiffHyperfeature[28], which fuses the time dimension with a set of learnable weights. Training is performed on the synthetic dataset GTAV[39]. Evaluation is performed on CityScapes[9].

Aggregation Method	Multi-step	w/. $\mathcal{V}_{t,l}^{\text{inter}}$	w/. $\mathcal{A}_{t,l}^{\text{cross}}$	mIoU (%) on CS
-	-	✓	-	49.72
-	-	✓	✓	51.09
Weighted Average	✓	✓	-	53.63
Weighted Average	✓	✓	✓	54.06
DIFF	✓	✓	-	53.21
DIFF	✓	✓	✓	54.80

Table 6: Implicit Knowledge Learning Study The baseline is set based on DIFF and timestep re-scheduling but without implicit knowledge learning. Training is performed on GTAV[39]. Evaluation is performed on CityScapes[9].

Implicit Knowledge Learning	$\mathcal{L}_{\text{consis}}$	mIoU (%) on CS
-	-	56.28
✓	w.o. $\mathcal{L}_{\text{consis}}$	44.82
✓	KL Loss	57.81
✓	L2 Loss	58.01

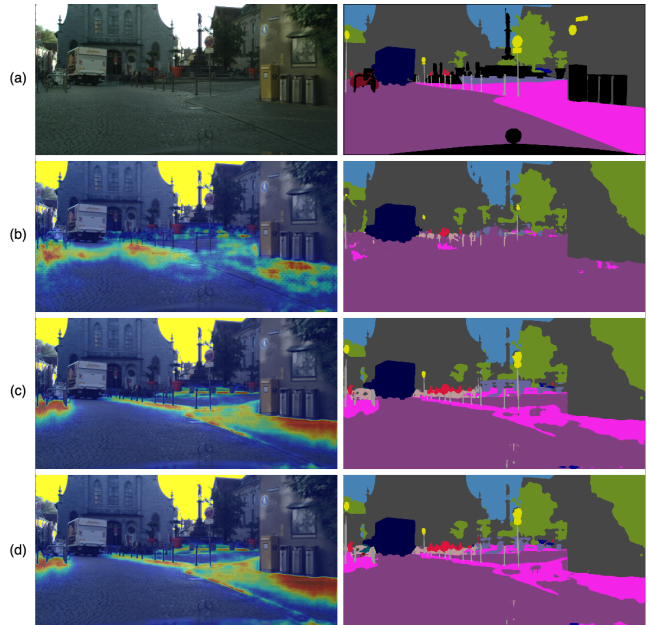


Figure 6: Comparison of prediction quality between (b) trained without implicit posterior knowledge learning (IPKL), (c) trained with IPKL but predicting without mask input, (d) trained with IPKL and predicting with mask input.

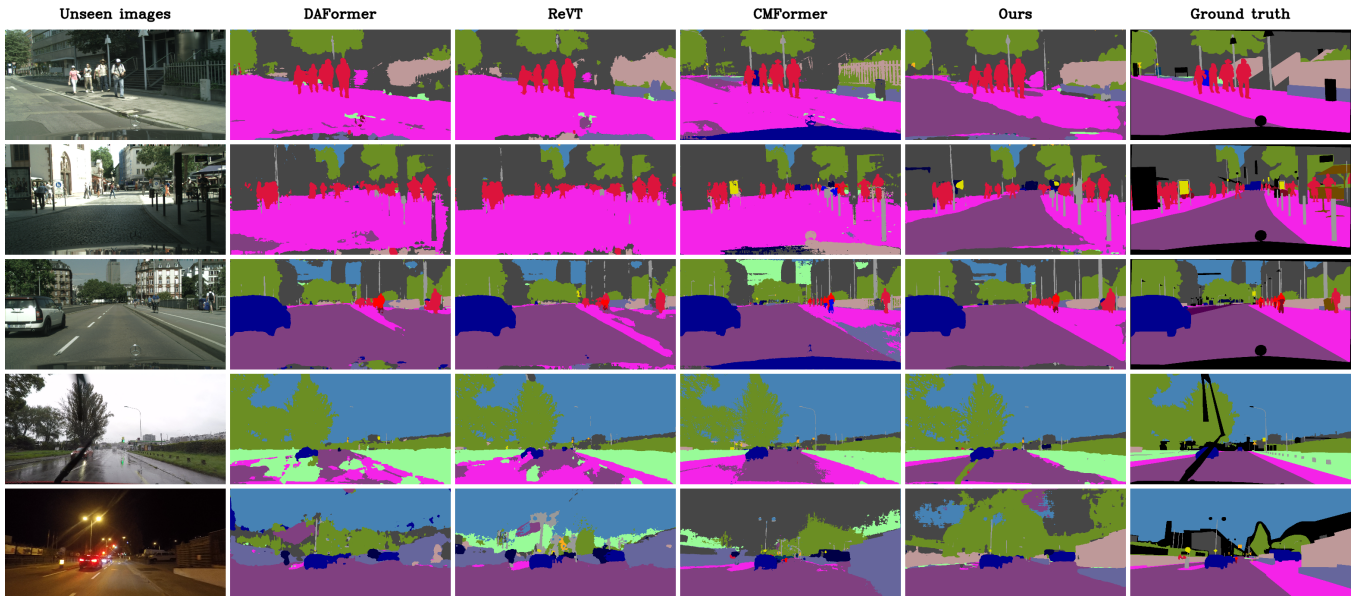


Figure 7: Unseen domain segmentation prediction of existing SOTA transformer-based domain generalization (DG) semantic segmentation methods (DAFormer[17], ReVT[49], CMFormer[4]) and our method. Training is performed on synthetic dataset GTAV[39]. Prediction is performed on five unseen real-world datasets.

difference in the conditional and unconditional branches. For the consistency loss function, we also try to use the KL divergence (Kullback–Leibler) [10] as the consistency training loss. The result indicates that this also benefits our dual-branch consistency learning; however, it may suffer from mode collapse during the training process.

On the other hand, we further analyze in depth the significance and implications of implicit posterior knowledge learning for domain generalization. As shown in Fig. 5, the results with implicit posterior knowledge training show a more significant improvement in some of the categories where there is an obvious degradation in cross-domain performance, like *sidewalk*, *wall*, *truck*, *bus*. One of the most noticeable boosts is in the category *sidewalk*, which brings +11% on mIoU. In this regard, we select an image from the validation set of CityScapes [9] to demonstrate the significance of implicit posterior knowledge learning for quality improvement. Fig. 6 provides the visual example of the attention on category *sidewalk* and final prediction of the segmentation model without IPKL training, the segmentation model with IPKL training and without mask reference input, the segmentation model with IPKL training and mask reference input respectively. With the attention paid to the real sidewalk region in the left-hand section, it can be noted that the model with IPKL training and mask reference input is more able to correctly discriminate the exact location and category on cross-domain compared to the model without IPKL training. Through the consistency training of IPKL, the model without mask reference input could also learn the vast majority of this ability, and shows a significant quality improvement in the prediction results across domains.

4.5 Quantitative Segmentation Results

Fig. 7 shows some visualized prediction results on unseen domain including CS, BDD, MV, ACDC, and DZ, comparing with the SOTA transformer-based backbone methods. Being trained on GTAV [39], our method shows better prediction quality in kinds of unknown scenarios, making correct predictions in categories that are confounded or unrecognized by other methods.

5 Conclusion

This paper delves into the potential of representations from pre-trained diffusion models in the challenging context of domain generalization for semantic segmentation. We propose Diffusion Feature Fusion (DIFF), an efficient block for extracting and fusing trajectory features of the diffusion process, which uniquely models cross-domain features by leveraging the rich prior knowledge of pre-trained diffusion models. We also explore the sampling of diffusion process, and introduce an implicit posterior knowledge learning framework, which is designed to learn the universal language perception of vision within conditional generation capabilities of diffusion models for further enhancing generalization ability. Extensive experiments on multiple settings demonstrated the superior performance of our method compared to the existing domain generalization semantic segmentation methods.

References

- [1] Omer Bar-Tal, Lior Yariv, Yaron Lipman, and Tali Dekel. 2023. MultiDiffusion: Fusing Diffusion Paths for Controlled Image Generation. In *International Conference on Machine Learning*. PMLR, 1737–1752.
- [2] Dmitry Baranchuk, Andrey Voynov, Ivan Rubachev, Valentin Khrukov, and Artem Babenko. 2021. Label-Efficient Semantic Segmentation with Diffusion Models. In *International Conference on Learning Representations*.
- [3] Georgios Batzolis, Jan Stanczuk, Carola-Bibiane Schönlieb, and Christian Etmann. 2021. Conditional image generation with score-based diffusion models. *arXiv preprint arXiv:2111.13606* (2021).
- [4] Qi Bi, Shaodi You, and Theo Gevers. 2024. Learning content-enhanced mask transformer for domain generalized urban-scene segmentation. In *Proceedings of the AAAI Conference on Artificial Intelligence*, Vol. 38. 819–827.
- [5] Chun-Fu Richard Chen, Quanfu Fan, and Rameswar Panda. 2021. Crossvit: Cross-attention multi-scale vision transformer for image classification. In *Proceedings of the IEEE/CVF international conference on computer vision*. 357–366.
- [6] Defang Chen, Zhenyu Zhou, Jian-Ping Mei, Chunhua Shen, Chun Chen, and Can Wang. 2023. A Geometric Perspective on Diffusion Models. *arXiv:2305.19947* [cs, stat]
- [7] Xinlei Chen, Zhuang Liu, Saining Xie, and Kaiming He. 2024. Deconstructing denoising diffusion models for self-supervised learning. *arXiv preprint arXiv:2401.14404* (2024).
- [8] Sungha Choi, Sanghun Jung, Huiwon Yun, Joanne T Kim, Seungryong Kim, and Jaegul Choo. 2021. Robustnet: Improving domain generalization in urban-scene segmentation via instance selective whitening. In *Proceedings of the IEEE/CVF Conference on Computer Vision and Pattern Recognition*. 11580–11590.
- [9] Marius Cordts, Mohamed Omran, Sebastian Ramos, Timo Rehfeld, Markus Enzweiler, Rodrigo Benenson, Uwe Franke, Stefan Roth, and Bernt Schiele. 2016. The cityscapes dataset for semantic urban scene understanding. In *Proceedings of the IEEE conference on computer vision and pattern recognition*. 3213–3223.
- [10] Thomas M Cover. 1999. *Elements of information theory*. John Wiley & Sons.
- [11] Yaroslav Ganin and Victor Lempitsky. 2015. Unsupervised domain adaptation by backpropagation. In *International conference on machine learning*. PMLR, 1180–1189.
- [12] Li Gao, Lefei Zhang, and Qian Zhang. 2021. Addressing domain gap via content invariant representation for semantic segmentation. In *Proceedings of the AAAI Conference on Artificial Intelligence*, Vol. 35. 7528–7536.
- [13] Rui Gong, Martin Danelljan, Han Sun, Julio Delgado Mangas, and Luc Van Gool. 2023. Prompting diffusion representations for cross-domain semantic segmentation. *arXiv preprint arXiv:2307.02138* (2023).
- [14] Rui Gong, Qin Wang, Dengxin Dai, and Luc Van Gool. 2022. One-shot domain adaptive and generalizable semantic segmentation with class-aware cross-domain transformers. *arXiv preprint arXiv:2212.07292* (2022).
- [15] Kaiming He, Xiangyu Zhang, Shaoqing Ren, and Jian Sun. 2016. Deep residual learning for image recognition. In *Proceedings of the IEEE conference on computer vision and pattern recognition*. 770–778.
- [16] Jonathan Ho, Ajay Jain, and Pieter Abbeel. 2020. Denoising diffusion probabilistic models. *Advances in neural information processing systems* 33 (2020), 6840–6851.
- [17] Lukas Hoyer, Dengxin Dai, and Luc Van Gool. 2022. Daformer: Improving network architectures and training strategies for domain-adaptive semantic segmentation. In *Proceedings of the IEEE/CVF Conference on Computer Vision and Pattern Recognition*. 9924–9935.
- [18] Jiaying Huang, Dayan Guan, Aoran Xiao, and Shijian Lu. 2021. Fsd: Frequency space domain randomization for domain generalization. In *Proceedings of the IEEE/CVF Conference on Computer Vision and Pattern Recognition*. 6891–6902.
- [19] Wei Huang, Chang Chen, Yong Li, Jiacheng Li, Cheng Li, Fenglong Song, Youliang Yan, and Zhiwei Xiong. 2023. Style projected clustering for domain generalized semantic segmentation. In *Proceedings of the IEEE/CVF conference on computer vision and pattern recognition*. 3061–3071.
- [20] Andrew Jaegle, Felix Gimeno, Andy Brock, Oriol Vinyals, Andrew Zisserman, and Joao Carreira. 2021. Perceiver: General perception with iterative attention. In *International conference on machine learning*. PMLR, 4651–4664.
- [21] Gihyun Kwon and Jong Chul Ye. 2023. Diffusion-based Image Translation using disentangled style and content representation. In *The Eleventh International Conference on Learning Representations, ICLR 2023*. The International Conference on Learning Representations.
- [22] Mingi Kwon, Jaeseok Jeong, and Youngjung Uh. 2022. Diffusion Models Already Have A Semantic Latent Space. In *The Eleventh International Conference on Learning Representations*.
- [23] Suhyeon Lee, Hongje Seong, Seongwon Lee, and Euntai Kim. 2022. WildNet: Learning domain generalized semantic segmentation from the wild. In *Proceedings of the IEEE/CVF conference on computer vision and pattern recognition*. 9936–9946.
- [24] Luping Liu, Yi Ren, Zhijie Lin, and Zhou Zhao. 2021. Pseudo Numerical Methods for Diffusion Models on Manifolds. In *International Conference on Learning Representations*.
- [25] Ilya Loshchilov and Frank Hutter. 2018. Decoupled Weight Decay Regularization. In *International Conference on Learning Representations*.
- [26] Cheng Lu, Yuhao Zhou, Fan Bao, Jianfei Chen, Chongxuan Li, and Jun Zhu. 2022. Dpm-solver: A fast ode solver for diffusion probabilistic model sampling in around 10 steps. *Advances in Neural Information Processing Systems* 35 (2022), 5775–5787.
- [27] Shilin Lu, Yanzhu Liu, and Adams Wai-Kin Kong. 2023. Tf-icn: Diffusion-based training-free cross-domain image composition. In *Proceedings of the IEEE/CVF International Conference on Computer Vision*. 2294–2305.
- [28] Grace Luo, Lisa Dunlap, Dong Huk Park, Aleksander Holynski, and Trevor Darrell. 2024. Diffusion hyperfeatures: Searching through time and space for semantic correspondence. *Advances in Neural Information Processing Systems* 36 (2024).
- [29] Fengmao Lv, Tao Liang, Xiang Chen, and Guosheng Lin. 2020. Cross-domain semantic segmentation via domain-invariant interactive relation transfer. In *Proceedings of the IEEE/CVF Conference on Computer Vision and Pattern Recognition*. 4334–4343.
- [30] Leland McInnes, John Healy, and James Melville. 2018. Umap: Uniform manifold approximation and projection for dimension reduction. *arXiv preprint arXiv:1802.03426* (2018).
- [31] Saeid Motiian, Marco Piccirilli, Donald A Adjeroh, and Gianfranco Doretto. 2017. Unified deep supervised domain adaptation and generalization. In *Proceedings of the IEEE international conference on computer vision*. 5715–5725.
- [32] Soumik Mukhopadhyay, Matthew Gwilliam, Vatsal Agarwal, Namitha Padmanabhan, Archana Swaminathan, Srinidhi Hegde, Tianyi Zhou, and Abhinav Shrivastava. 2023. Diffusion Models Beat GANs on Image Classification. *arXiv:2307.08702* [cs]
- [33] Hyeonseob Nam, HyunJae Lee, Jongchan Park, Wonjun Yoon, and Donggeun Yoo. 2021. Reducing domain gap by reducing style bias. In *Proceedings of the IEEE/CVF Conference on Computer Vision and Pattern Recognition*. 8690–8699.
- [34] Gerhard Neuhold, Tobias Ollmann, Samuel Rota Buló, and Peter Kontschieder. 2017. The mapillary vistas dataset for semantic understanding of street scenes. In *Proceedings of the IEEE international conference on computer vision*. 4990–4999.
- [35] Xingang Pan, Ping Luo, Jianping Shi, and Xiaoou Tang. 2018. Two at once: Enhancing learning and generalization capacities via ibn-net. In *Proceedings of the european conference on computer vision (ECCV)*. 464–479.
- [36] Duo Peng, Ping Hu, Qiuhong Ke, and Jun Liu. 2023. Diffusion-based image translation with label guidance for domain adaptive semantic segmentation. In *Proceedings of the IEEE/CVF International Conference on Computer Vision*. 808–820.
- [37] Duo Peng, Yinjie Lei, Munawar Hayat, Yulan Guo, and Wen Li. 2022. Semantic-aware domain generalized segmentation. In *Proceedings of the IEEE/CVF conference on computer vision and pattern recognition*. 2594–2605.
- [38] Duo Peng, Yinjie Lei, Lingqiao Liu, Pingping Zhang, and Jun Liu. 2021. Global and local texture randomization for synthetic-to-real semantic segmentation. *IEEE Transactions on Image Processing* 30 (2021), 6594–6608.
- [39] Stephan R Richter, Vibhav Vineet, Stefan Roth, and Vladlen Koltun. 2016. Playing for data: Ground truth from computer games. In *Computer Vision—ECCV 2016: 14th European Conference, Amsterdam, The Netherlands, October 11–14, 2016, Proceedings, Part II 14*. Springer, 102–118.
- [40] Robin Rombach, Andreas Blattmann, Dominik Lorenz, Patrick Esser, and Björn Ommer. 2022. High-resolution image synthesis with latent diffusion models. In *Proceedings of the IEEE/CVF conference on computer vision and pattern recognition*. 10684–10695.
- [41] Olaf Ronneberger, Philipp Fischer, and Thomas Brox. 2015. U-net: Convolutional networks for biomedical image segmentation. In *Medical image computing and computer-assisted intervention—MICCAI 2015: 18th international conference, Munich, Germany, October 5–9, 2015, proceedings, part III 18*. Springer, 234–241.
- [42] German Ros, Laura Sellart, Joanna Materzynska, David Vazquez, and Antonio M Lopez. 2016. The synthia dataset: A large collection of synthetic images for semantic segmentation of urban scenes. In *Proceedings of the IEEE conference on computer vision and pattern recognition*. 3234–3243.
- [43] Dan Ruta, Gemma Canet Tarres, Alexander Black, Andrew Gilbert, and John Collomosse. [n. d.]. ALADIN-NST: Self-supervised disentangled representation learning of artistic style through Neural Style Transfer. ([n. d.]).
- [44] Christos Sakaridis, Dengxin Dai, and Luc Van Gool. 2019. Guided curriculum model adaptation and uncertainty-aware evaluation for semantic nighttime image segmentation. In *Proceedings of the IEEE/CVF International Conference on Computer Vision*. 7374–7383.
- [45] Christos Sakaridis, Dengxin Dai, and Luc Van Gool. 2021. ACDC: The adverse conditions dataset with correspondences for semantic driving scene understanding. In *Proceedings of the IEEE/CVF International Conference on Computer Vision*. 10765–10775.
- [46] Jiaming Song, Chenlin Meng, and Stefano Ermon. 2020. Denoising Diffusion Implicit Models. In *International Conference on Learning Representations*.
- [47] Yang Song, Jascha Sohl-Dickstein, Diederik P Kingma, Abhishek Kumar, Stefano Ermon, and Ben Poole. 2020. Score-Based Generative Modeling through Stochastic Differential Equations. In *International Conference on Learning Representations*.
- [48] Luming Tang, Menglin Jia, Qianqian Wang, Cheng Perng Phoo, and Bharath Hariharan. 2023. Emergent correspondence from image diffusion. *Advances in Neural Information Processing Systems* 36 (2023), 1363–1389.

- [49] Jan-Aike Termöhlen, Timo Bartels, and Tim Fingscheidt. 2023. A Re-Parameterized Vision Transformer (ReVT) for Domain-Generalized Semantic Segmentation. In *Proceedings of the IEEE/CVF International Conference on Computer Vision*. 4376–4385.
- [50] Wilhelm Tranheden, Viktor Olsson, Juliano Pinto, and Lennart Svensson. 2021. Dacs: Domain adaptation via cross-domain mixed sampling. In *Proceedings of the IEEE/CVF Winter Conference on Applications of Computer Vision*. 1379–1389.
- [51] Ashish Vaswani, Noam Shazeer, Niki Parmar, Jakob Uszkoreit, Llion Jones, Aidan N Gomez, Lukasz Kaiser, and Illia Polosukhin. 2017. Attention is all you need. *Advances in neural information processing systems* 30 (2017).
- [52] Jindong Wang, Cuiling Lan, Chang Liu, Yidong Ouyang, Tao Qin, Wang Lu, Yiqiang Chen, Wenjun Zeng, and Philip Yu. 2022. Generalizing to unseen domains: A survey on domain generalization. *IEEE Transactions on Knowledge and Data Engineering* (2022).
- [53] Jinglong Wang, Xiawei Li, Jing Zhang, Qingyuan Xu, Qin Zhou, Qian Yu, Lu Sheng, and Dong Xu. 2023. Diffusion model is secretly a training-free open vocabulary semantic segmenter. *arXiv preprint arXiv:2309.02773* (2023).
- [54] Qiucheng Wu, Yujian Liu, Handong Zhao, Ajinkya Kale, Trung Bui, Tong Yu, Zhe Lin, Yang Zhang, and Shiyu Chang. 2023. Uncovering the disentanglement capability in text-to-image diffusion models. In *Proceedings of the IEEE/CVF Conference on Computer Vision and Pattern Recognition*. 1900–1910.
- [55] Enze Xie, Wenhai Wang, Zhiding Yu, Anima Anandkumar, Jose M Alvarez, and Ping Luo. 2021. SegFormer: Simple and efficient design for semantic segmentation with transformers. *Advances in neural information processing systems* 34 (2021), 12077–12090.
- [56] Jiarui Xu, Sifei Liu, Arash Vahdat, Wonmin Byeon, Xiaolong Wang, and Shalini De Mello. 2023. Open-vocabulary panoptic segmentation with text-to-image diffusion models. In *Proceedings of the IEEE/CVF Conference on Computer Vision and Pattern Recognition*. 2955–2966.
- [57] Fisher Yu, Haofeng Chen, Xin Wang, Wenqi Xian, Yingying Chen, Fangchen Liu, Vashisht Madhavan, and Trevor Darrell. 2020. Bdd100k: A diverse driving dataset for heterogeneous multitask learning. In *Proceedings of the IEEE/CVF conference on computer vision and pattern recognition*. 2636–2645.
- [58] Xiangyu Yue, Yang Zhang, Sicheng Zhao, Alberto Sangiovanni-Vincentelli, Kurt Keutzer, and Boqing Gong. 2019. Domain randomization and pyramid consistency: Simulation-to-real generalization without accessing target domain data. In *Proceedings of the IEEE/CVF International Conference on Computer Vision*. 2100–2110.
- [59] Wenliang Zhao, Yongming Rao, Zuyan Liu, Benlin Liu, Jie Zhou, and Jiwen Lu. 2023. Unleashing text-to-image diffusion models for visual perception. In *Proceedings of the IEEE/CVF International Conference on Computer Vision*. 5729–5739.
- [60] Yuyang Zhao, Zhun Zhong, Na Zhao, Nicu Sebe, and Gim Hee Lee. 2022. Style-hallucinated dual consistency learning for domain generalized semantic segmentation. In *European conference on computer vision*. Springer, 535–552.
- [61] Zhun Zhong, Yuyang Zhao, Gim Hee Lee, and Nicu Sebe. 2022. Adversarial style augmentation for domain generalized urban-scene segmentation. *Advances in Neural Information Processing Systems* 35 (2022), 338–350.
- [62] Kaiyang Zhou, Ziwei Liu, Yu Qiao, Tao Xiang, and Chen Change Loy. 2023. Domain Generalization: A Survey. *IEEE Transactions on Pattern Analysis & Machine Intelligence* 45, 04 (2023), 4396–4415.